

Synthesis and characterization of supported Phenolic resin/Carbon nanotubes Carbon membranes for gas separation

Morteza Afsari¹; Morteza Asghari^{1, 2*}; Payam Mohammadi Moghaddam²

¹Separation Processes Research Group (SPRG), Department of Engineering, University of Kashan, Kashan, Iran

²Department of Chemical Engineering, Science and Research Branch, Islamic Azad University, Shiraz, Iran

Received 21 May 2017; revised 30 July 2017; accepted 22 August 2017; available online 28 August 2017

Abstract

In this work, separation performance of supported carbon membranes produced from Novolac Phenolic resin as the main precursor and carbon nanotubes as nanofiller were investigated for separation of CO₂ from N₂ and CH₄. Supports were produced by carbonization of Novolac Phenolic resin-activated carbon mixture, and selective layer was coated by dip coating of prepared supports into solutions with different concentrations of Novolac Phenolic resin/carbon nanotubes. The composite membranes were pre-oxidized and carbonized under vacuum condition up to 160 °C and 700 °C, respectively. Carbon membranes were characterized using FE-SEM, BET, and gas permeation test. Results revealed that the best proportion of Novolac Phenolic resin/activated carbon was 40/60 wt% to make a defect-free and applicable support, most pores of which had sizes less than 10 nm. Membranes were tested at different pressures, and the results showed that CO₂ permeability increased with pressure. The carbon membrane made with 40 wt% Novolac phenolic resin and 1 wt% carbon nanotubes showed the best separation performance with CO₂/CH₄ and CO₂/N₂ selectivity of 19.5 and 18.3 in 10 bar, respectively.

Keywords: Carbon Membrane; Phenolic Resin; Carbon Nanotube; Carbonization; Gas Separation.

How to cite this article

Afsari M, Asghari M, Mohammadi Moghaddam P. Synthesis and characterization of supported Phenolic resin/Carbon nanotubes Carbon membranes for gas separation. *Int. J. Nano Dimens.*, 2017; 8 (4): 316-328.

INTRODUCTION

Membrane separation has attracted the interest of researchers for gas separation processes due to its beneficence and efficiency in industrial applications [1, 2]. Current studies revealed that, compared to polymeric membranes, inorganic membranes show high performance in CO₂ separation from natural gas or flue gas, especially in corrosive or high temperature conditions [3, 4]. Carbon membranes are a type of inorganic membranes; primary studies have demonstrated privileges like high selectivity based on molecular shape, high hydrophobicity, as well as good thermal resistivity, making it suitable nominee for gas separation processes [5-7] heavy hydrocarbon recovery, water dehydration as well as nitrogen and helium separation. In particular, the current commercial membrane materials for CO₂ removal (cellulose acetate, polyimides and perfluoropolymers).

In order to produce high performance carbon membranes, different thermosetting polymers have been tried, including poly acrylonitrile [7, 8], phenolic resin [9, 10], polyimide [11, 12], and coal tar pitch [13].

Phenolic resin is one of the most popular and inexpensive polymers used in a wide range of applications such as commodity construction materials [9]. A few works have investigated the use of phenolic resin as precursor of carbon membranes. Tennisson *et al.* described the preparation of carbon membranes produced by carbonization of phenolic resin and supported on highly permeable Novolac resin macro porous support with H₂/CH₄ permselectivities in the ranges of 2 (at 238 °C) to 20 (550 °C) [14]. Also Shusen *et al.* prepared an asymmetric carbon membrane, prepared by pyrolysis of phenolic resin in temperature range of 800-950 °C, revealing a permselectivity of 10.6 at ambient temperature

* Corresponding Author Email: asghari@kashanu.ac.ir

for the O₂/N₂ system [14, 15] appropriate for gas separation applications, was made through carbonization at 800 °C of a precursor structure containing two phenol-formaldehyde resins, a partially cured novolac resin in 30 μm grains (bulk material). In addition to excellent properties of carbon membranes, the main problem of carbon membranes is their brittleness which makes difficulty in their industrial application, thus the first step of this work emphasized on production of a smooth and stiff support from NPR-based mixture. Then to find a comprehensive procedure for obtaining efficient and defect-free surface layer, different concentrations of phenolic resin solutions were coated on prepared supports. Support and selective layers were produced from the same material to decrease differences in expansion factors. Furthermore, studies showed that incorporation of nanofillers like carbon nanotubes, can improve the performance of produced carbon membranes [16, 17], but the effect of their incorporation in Phenolic resin carbon membranes has not been reported yet. Multi wall carbon nanotube was used to investigate its effect on the performance of produced carbon membranes. To determine the influence of operational condition on performance of membranes, the effect of pressure difference on the permeability and selectivity of membranes was also investigated.

EXPERIMENTAL

Preparation of support

To find a support with best quality, three different mixtures were prepared as following: Novolac Phenolic resin (NPR) and activate carbon powder, respectively purchased from Moheb and Loba company, mixed with different proportions (50/50, 60/40 and 70/30 wt. %), and then some drops of ethanol (Merck) were added to dissolve NPR. The mixtures were sorely stirred and dried in room temperature and then were pulverized and sieved with fine-mesh sieve. Then derived powder was pressed in a disc shaped mold under 160 KN force hydraulic press to produce a disc shape support. Carbonization process was carried out to 700 °C to form carbonized support. Table 1 shows the classification and ingredient proportion of mixtures.

Preparation of selective layer

The separation process was carried out by

selective layer, and efficiency of process directly depends on quality of this layer [18, 19] and they play an increasingly important role in reducing the environmental impacts and costs of many industrial processes. This book describes recent and emerging results in membrane gas separation, including highlights of nanoscience and technology, novel polymeric and inorganic membrane materials, new membrane approaches to solve environmental problems e.g. greenhouse gases, aspects of membrane engineering, and recent achievements in industrial gas separation. It includes: Hyperbranched polyimides, amorphous glassy polymers and perfluorinated copolymers Nanocomposite (mixed matrix. Three different solutions were prepared by addition of 20, 40, and 60 wt% of NPR to ethanol. Solutions sorely stirred on magnetic stirrer and in room temperature for about 2 hour. Then, the solutions were degassed and dip coated on produced supports. All prepared samples were heated up to 160 °C for pre-oxidation step and then heated to 700 °C in vacuum for pyrolysis step, with heating rate of 1 °C/min.

In order to prepare CNT-contained carbon membranes, Multi walled CNT (MWCNT), bought from Notrino with inner diameters of 2-5 nm, were dissolved in ethanol, sonicated for 30 minutes, and then NPR was added to prepare composite membranes with desired concentration of NPR and 1 wt% CNT. Generally, six mixtures were prepared and nominated as following: C20 (20 wt% NPR), C20M (20 wt% NPR+ 1 wt% MWCNT), C40 (40 wt% NPR), C40M (40 wt% NPR+ 1 wt% MWCNT), and C60 (60 wt% NPR). Fig. 1 shows temperature change versus time for both pre-oxidation and pyrolysis step.

Characterization of CMS membranes

The structures of supported carbon membranes were compared with photos captured by high resolution macro photo camera. Also, the microscopic description of the membranes was shown with scanning electron microscopy (SEM). The cross section and surface morphology of the membranes were observed through MIRA3 TESCANA (Czech Republic), field emission scanning electron microscope at 15kV. Pore structure of the support was explored with BET test. Finally, gas permeation test was carried out to compare the selectivity and permeability of membranes. Also, XRD analysis was carried out to investigate the crystallinity of samples. FTIR analysis was

performed using Nicolet-550 device in ambient temperature at wave number range of 400–4000 cm⁻¹. Three gases were chosen for estimation of separation characteristics of membranes with the following critical dimension: N₂ (3.64 Å), CH₄ (3.8 Å), and CO₂ (3.3 Å). To reduce the side effects of permeated gas on the membranes, tests were carried out on gas sizes. Permeance and selectivity of membranes can be calculated according to the following correlations:

$$\frac{P}{l} = \frac{Q}{\Delta p \cdot A} [\text{mol/m}^2 \cdot \text{s} \cdot \text{Pa}] \quad (1)$$

$$S_{A/B} = \frac{P_A}{P_B} = \frac{(P/l)_A}{(P/l)_B} \quad (2)$$

Where, Q is volumetric flowrate (mol/s); Δp is pressure difference in sides of membrane (Pa); A is surface area (m²) of membrane, and P/l is permeance of the membrane.

RESULTS AND DISCUSSION

Macro photos of supports

Macro photos of manufactured supports with different percentages of NPR are shown in Table 2. Supports prepared with mixture of 60% activated carbon and 40% NPR showed adequate quality. BET test also approved the results. So, this support

was selected for carbon membrane preparation.

FE-SEM

Fig. 2 (a, b and c) show FESEM of support surface. Fig. 3 (a, b) show FE-SEM images of C20M carbon membrane. Images show that carbon membrane produced with 20 wt% NPR has some crack on the surface in dimension of 0.5-7 μm. These defects can reduce the efficiency and selectivity of membrane.

Fig. 4 (a, b) shows the FESM images of carbon membrane produced from 40 wt% NPR (C40). Fig. 4(a) shows that a faultless carbonized selective layer is achievable by carbonization of 40 wt% NPR solution. Fig. 4(b) shows the cross sectional view of C40. It is observed that the average thickness of selective layer is about 5 μm. Low thickness of membrane is one of the most important privileges of produced membrane which may gain high gas flux in addition to reasonable selectivity.

Fig. 5 (a, b and c) shows the images of CNT-containing carbon membrane (C40M) in three resolutions of 2 μm (a), 500 nm (b) and 200 nm (c); however, efforts for homogenous distribution of CNT in NPR solution in some sections of CNT have aggregated. More homogenous distribution could be expected by more powerful ultrasonic bath or some other methods for CNT dispersion [1].

Table 1: Ingredient and their proportion in preparation of support.

Comparison after pyrolysis	NPR Wt%	Activated carbon Wt%	Classification
Some crack formed in surface	70	30	Mixture 1
High quality and adamant	60	40	Mixture 2
Brittle	50	50	Mixture 3

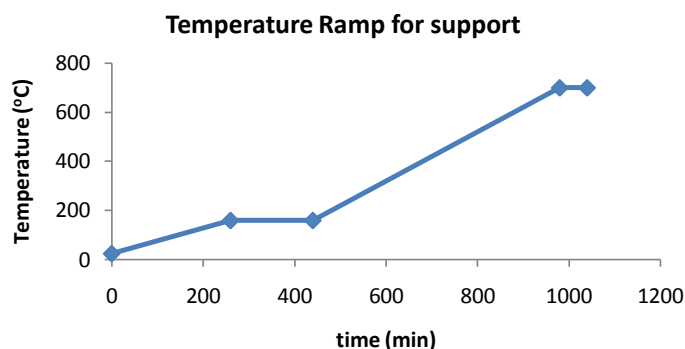


Fig. 1: Temperature change of supported membranes in pre-oxidation and pyrolysis step (rate of 1 °C/min in vacuum condition).

Table 2: Macro photos of supports.

Supports			
NPR (%Wt)	30%	40%	50%

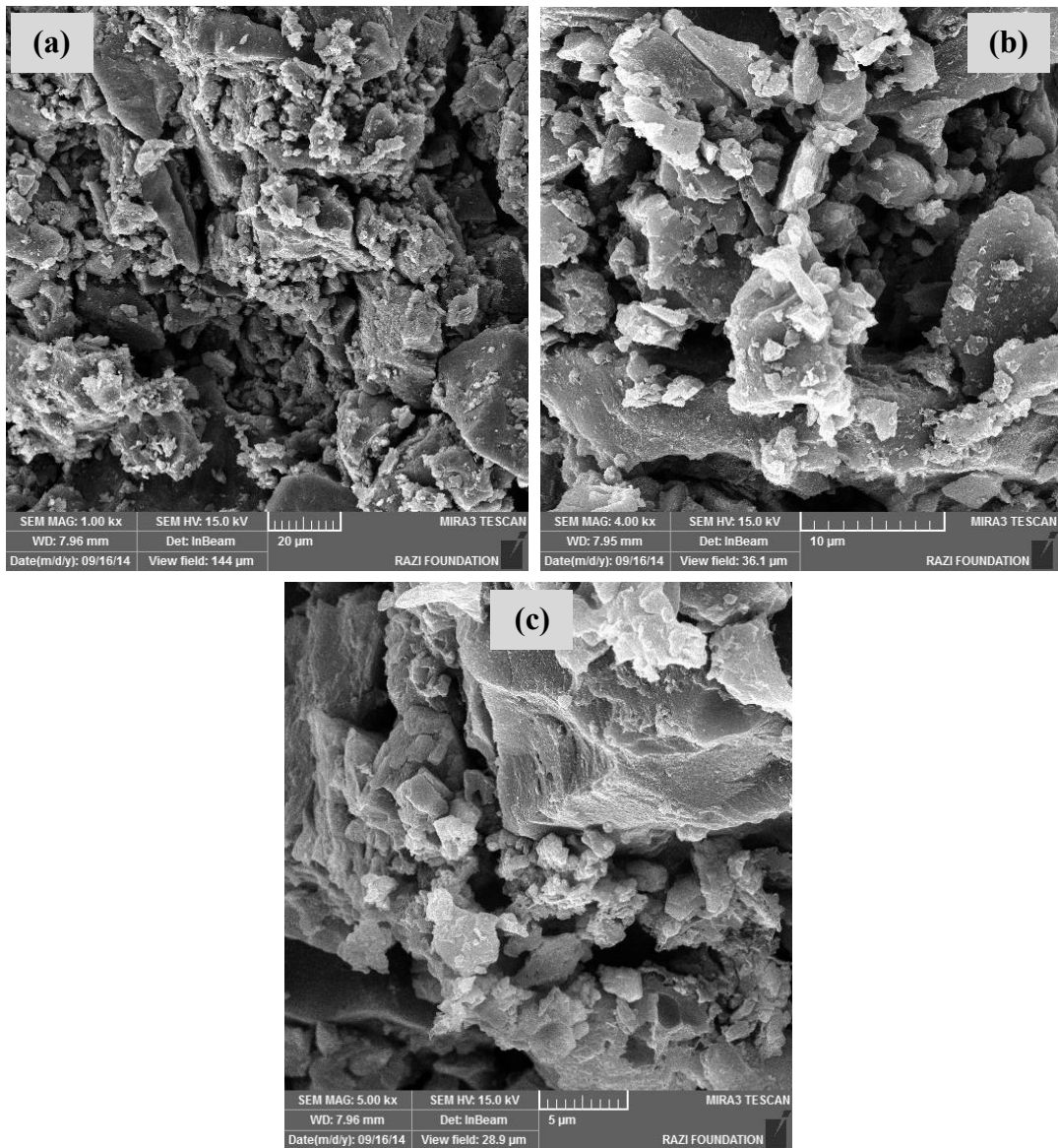


Fig. 2: FE-SEM images of carbonized support a) 20 µm, b) 10 µm, c) 5µm.

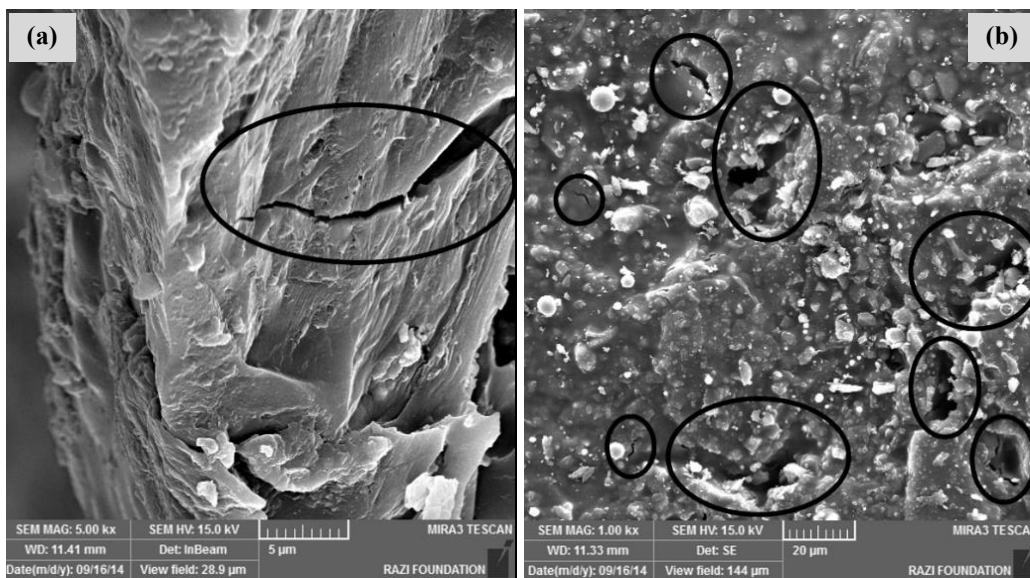


Fig. 3: FE-SEM images of C20M a) cross sectional view, b) surface view.

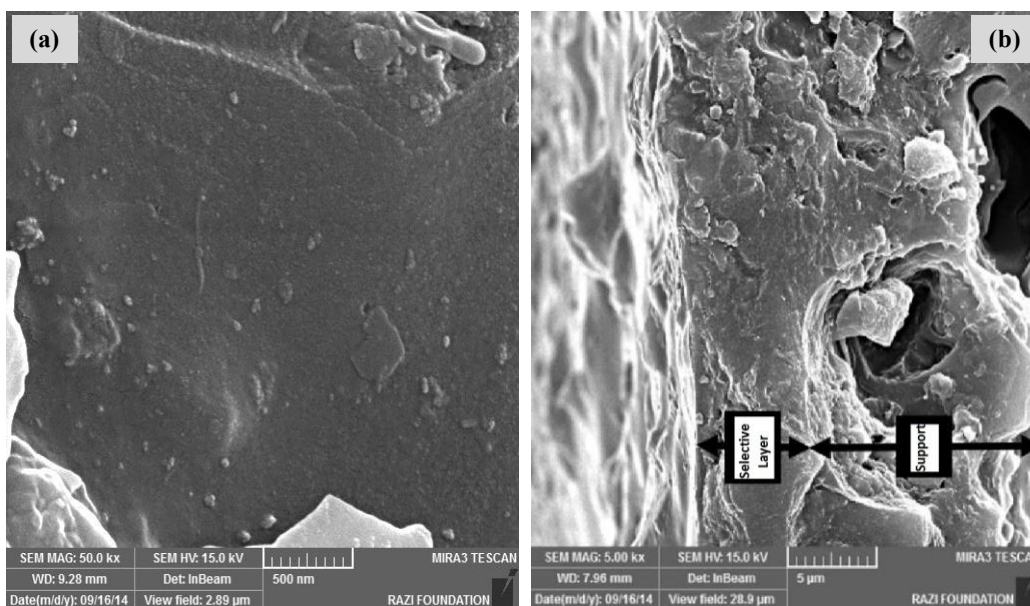


Fig. 4: FE-SEM images C40 a) surface view, b) cross sectional view.

BET test

BET test gives an isothermal curve which could be used to determine the pore size distribution of supports. Isothermal curves were compared with pre-specified standard curves (Fig. 6 (a, b)).

Adsorption curves of BET test for prepared support with 60% activated carbon and 40% NPR are shown in Fig. 7. In BET analyzes, both isothermal adsorption and desorption test were carried out. Comparisons of BET test with standard patterns

revealed that the derived isothermal curve of adsorption and desorption obey from standard curve I. Also comparison of derived hysteresis loop with standard patterns showed that this loop coincided with H_4 loop. Samples with adsorption pattern I and hysteresis loop H_4 are classified in micro-porous category. Fig. 8 qualifies these statements by drawing pore size distribution of prepared support. Most pores had diameter less than 10 nm. It is obviously clear that the prepared

support is suitable for coating of selective layer and approves the results of macro photos.

Weight change of samples after heat treatment

Table 3 contains data about weight changes of samples before and after heat treatments in pre-oxidation and pyrolysis steps. Sample investigation revealed that average weight loss during pre-oxidation process is about 3.5% and during pyrolysis is about 22%. These weight losses belong to cross sectional junction of Novolac Resin and removal of non-carbonic substances.

Gas test results

A schematic illustration of the gas permeation test setup is presented in Fig. 9.

Fig. 10 (a, b and c) illustrate the permeability change of different gases as a function of feed

pressure for all prepared carbon membranes. Accordingly, CO₂ permeability in all membranes increases with feed pressure. Fig. 10 (b and c) show the effect of pressure on N₂ and CH₄ gases, respectively; the permeability for all membranes with respect to pressure is relatively constant.

Many previous studies have proved this trend of permeability and selectivity behavior for separation of more adsorbable gases from less adsorbable gases in both carbon and zeolite-based membranes [21-23]. Mechanism of transport through these membranes can occur with selective surface flow [24, 25]. Hereby, more adsorbable gas is adsorbed on the surface of pores, diffused through it, and desorbed on the other side of membranes. CO₂ permeation is greater because of more tendency of CO₂ for adsorption on surface and its lower dynamic size relative to N₂ and

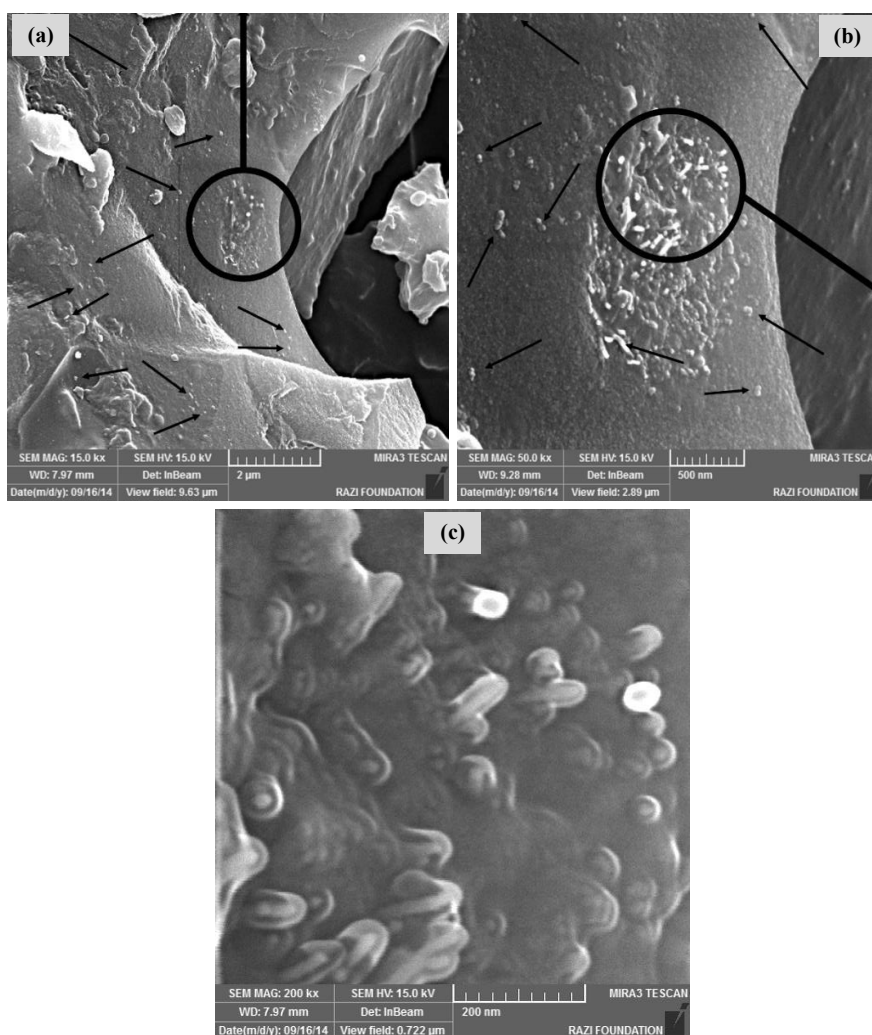


Fig. 5: Schematic of CNTs position inside carbon membrane C40M by FE-SEM images a) 2μm, b) 500 nm, c) 200 nm.

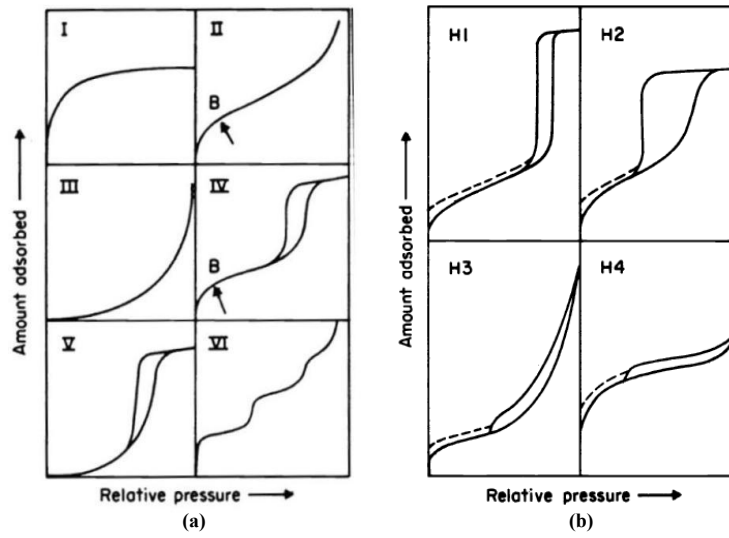


Fig. 6: Different types of a) adsorption and desorption isothermal curve, b) hysteresis loop [20].

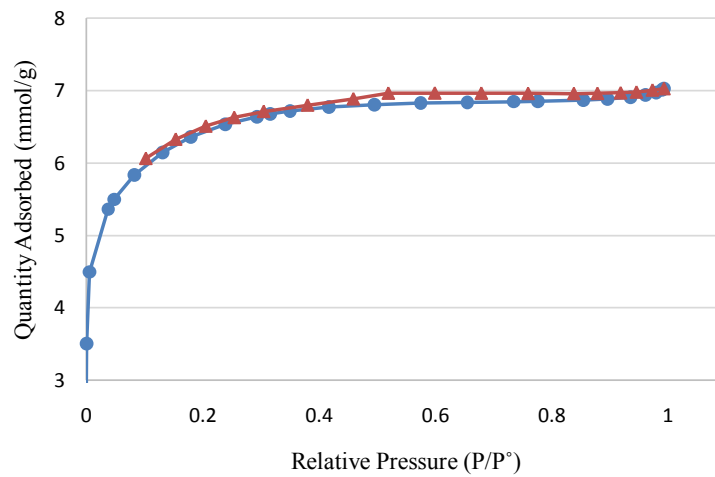


Fig. 7: N_2 isothermal adsorption and desorption.

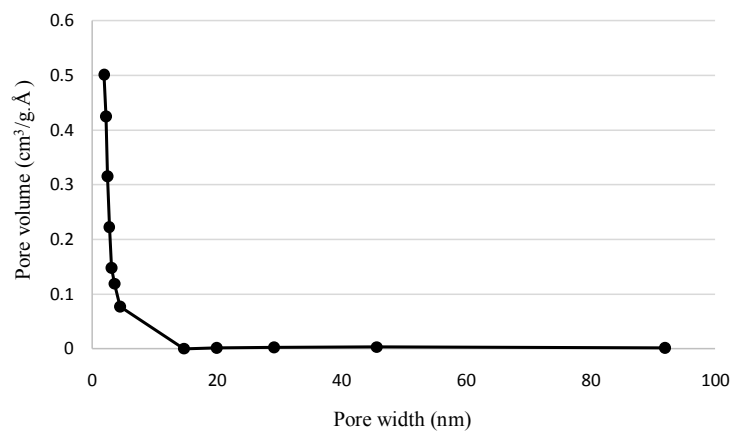


Fig. 8: Pore size distribution of carbon membrane.

Table 3: Sample weighting in different membrane preparation step.

Sample number	sample weight	Weight after pre-oxidation	Weight loss after pre-oxidation (%)	Weight after pyrolysis	Weight loss After pyrolysis (%)	
Support	A	1.163	1.150	1.12	0.909	21.84
C40	C	1.164	1.151	1.12	0.931	20.02
C40M	E	1.164	1.152	1.03	0.919	21.05

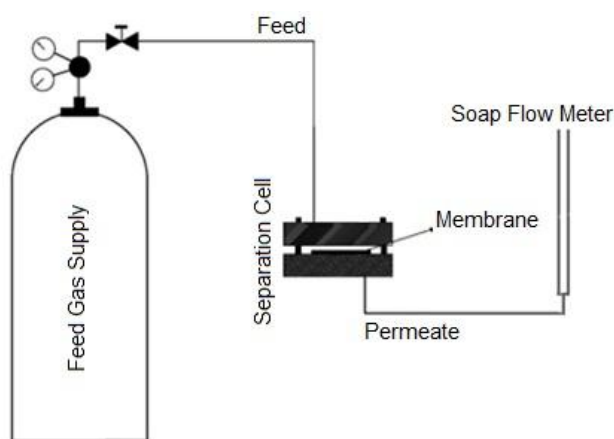


Fig. 9: Membrane test setup.

CH_4 . On the other hand, nonadsorbable or less adsorbable gases pass through pores only with pressure driving force; therefore, the permeation rate of CO_2 is higher than others. Overall, the mechanism of transport depends on the pore size and size of molecules and varies from molecular sieving, selective diffusion, Knudsen flow, or viscous flow. According to gas permeation results and mean free path of gases which vary from 4 to 50 nm, it can be concluded that the permeation of gas through produced carbon membranes may occur with selective surface flow or Knudsen flow, depending on the size of pores. In general, more exact and special experiments should be carried out to accurately determine the mechanism of transport.

Fig. 11 shows CO_2/CH_4 and CO_2/N_2 selectivity for different membranes. C40M and C40 showed better separation performance. CO_2/CH_4 selectivity for C40M rose to more than 18, while it was about 13 for C40 membranes values. The presence of CNTs in C40M enhanced permeabilities for all gases, compared to C40, but CNT had more powerful impact on CO_2 separation. CNT could strengthen the membrane

and decrease the defects and cracks of carbon membrane, so it could enhance the quality of membrane. Furthermore, CO_2 had lower dynamic diameter and higher adsorption tendency and was adsorbed with CNTs and diffuses through it; these factors highly affected CO_2 permeability. For CH_4 and N_2 , only the size of molecules influenced the diffusion, and their diffusion rate was almost in the same order and was less than CO_2 .

Other membranes rendered selectivities less than six. Carbon membranes produced by 60wt% NPR had some cracks on their surface, and as a result, the selectivity dramatically decreased for C60 membrane.

FTIR

FTIR analysis has been broadly used to investigate the chemical structure and formation of bonds in prepared membranes. Fig. 12 (a, b and c) show the FTIR spectrum for neat Novolac, CNT, and carbonized novolac samples. According to the Fig. 12 (a), the bonds in wavenumbers below 850 cm^{-1} are related to the benzene of Novolac phenolic resin. the bending and asymmetric bending vibration peaks of C-H bonds of methyl

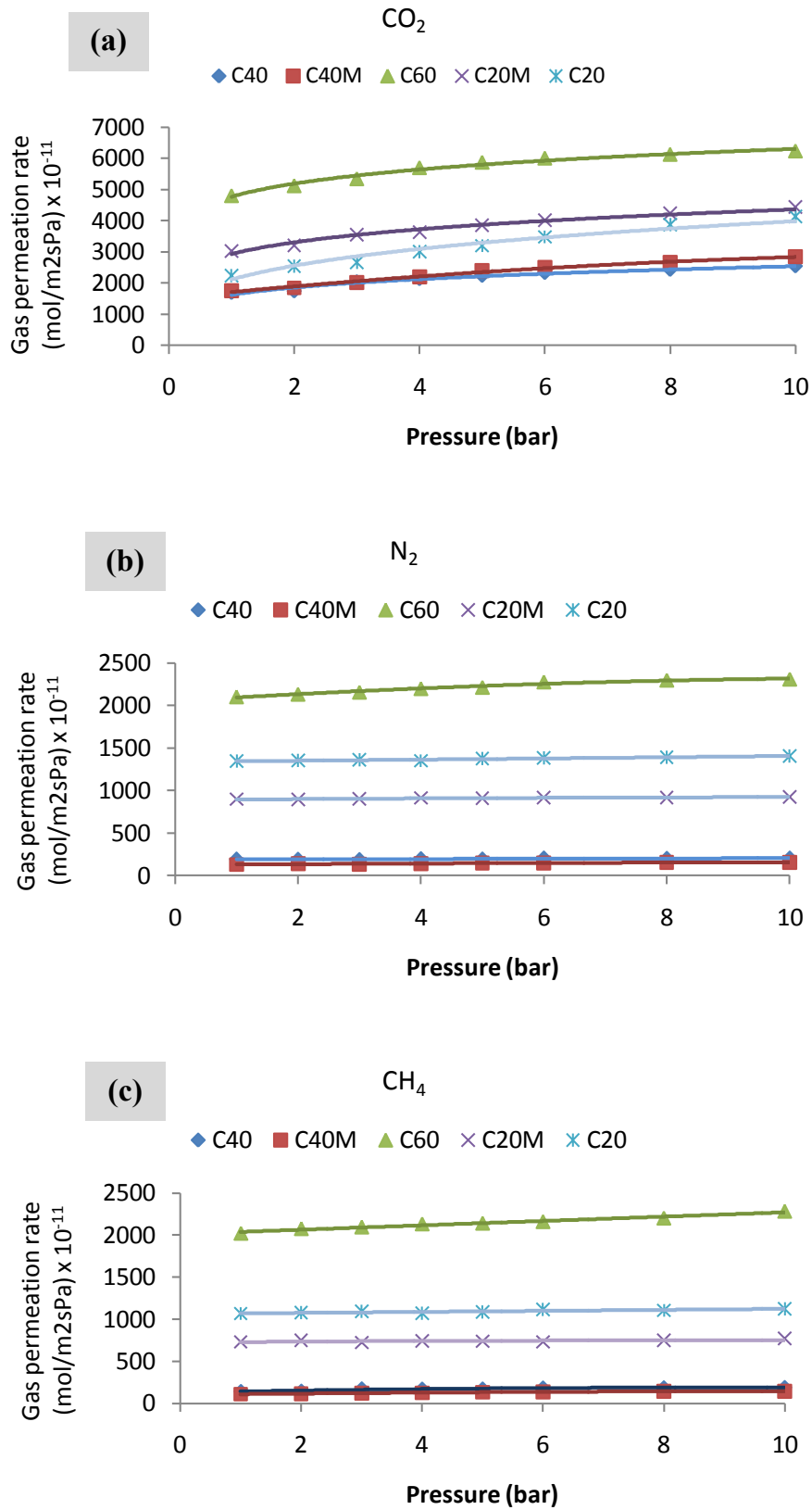


Fig. 10: Permeability change versus pressure on prepared carbon membranes for different gases a) CO₂, b) N₂, c) CH₄.

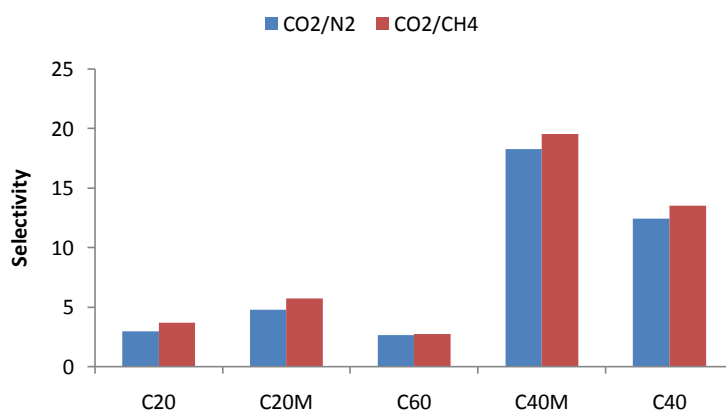
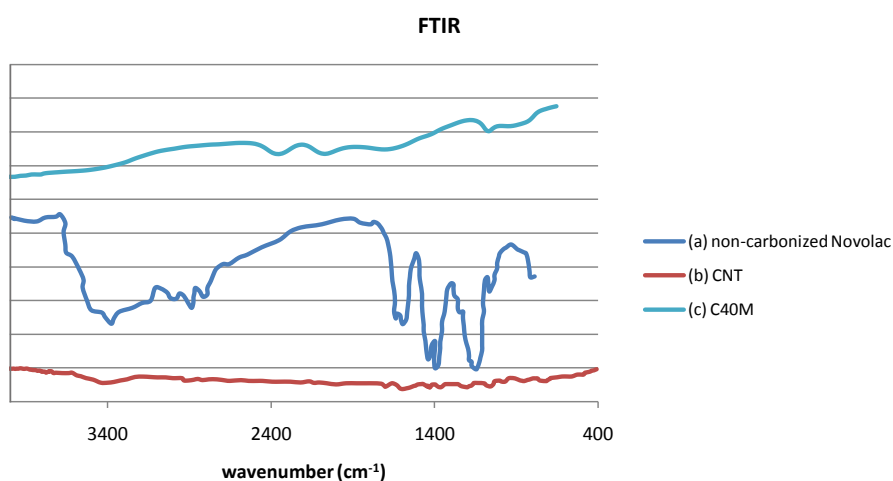
Fig. 11: CO₂/CH₄ and CO₂/N₂ Selectivity for manufactured membranes.

Fig. 12: FTIR patterns for (a) non-carbonized Novolac, (b) MWCNT, (c) C40M membrane.

and methylene groups can be respectively detected around 1242 and 1475 cm⁻¹ [26, 27]. Also the peaks at 2915 and 3020 cm⁻¹ are related to the both symmetric and asymmetric C-H stretching vibration. The peak related to vibration of C=C bonds in Novolac resin is located at 1665 cm⁻¹. Overall the peaks in narrow range of 2800-3000 cm⁻¹ are assigned to C-O vibration and C=C stretching vibration of phenol groups of Novolac [10, 27]. According to Fig. 12 (b), The C=C and C=O bonds of Carbon nanotube have shown two main peaks placed at 1610 and 1700 cm⁻¹, which reveals significant formation of crosslinks. The stretching vibration of O-H could be seen at 3448 cm⁻¹ [28, 29, 30].

Comparison of FTIR Fig. 12 (a and c) show that OH stretching vibration has been significantly changed after carbonization of NPR. Neat Novolac showed OH bond near 3400 cm⁻¹ while

it disappeared after carbonization. This change demonstrates the elimination of OH groups in pyrolysis step. Additionally, peaks around 2900 which belong to methyl and methylene groups were eliminated after carbonization. This change can be attributed to elimination of methyl and methylene groups [31, 32].

The neat resin shows some peaks in the range of 1400-1500 cm⁻¹ which was changed after carbonization. The carbonized samples show a peak around 1400 which can be attributed to symmetrical deformation bond of C-H. The overall consideration to peaks of methylene show that carbonization dramatically destruct the methylene bridges. Also the location of oxygen group band around 1300 cm⁻¹ have changed and went to lower wave numbers (around 1200 cm⁻¹) after carbonization which show change in structure of oxygen groups [26, 33].

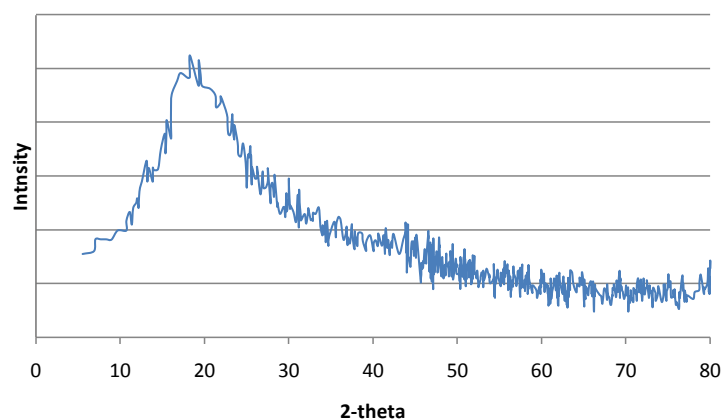


Fig. 13: XRD patterns for non-carbonized Novolac.

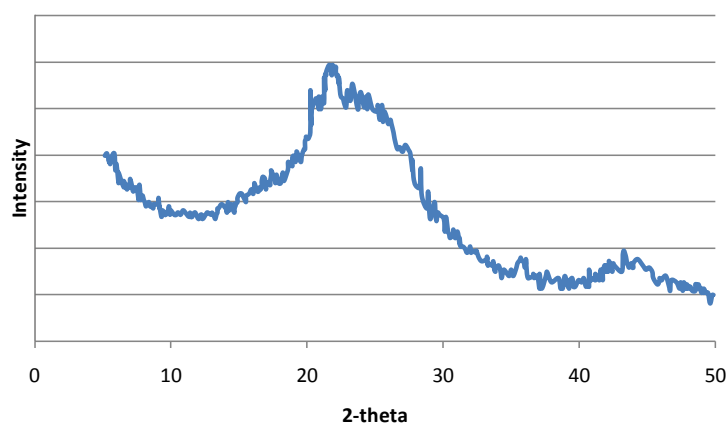


Fig. 14: XRD patterns for carbonized Novolac (C40M).

XRD

XRD is a qualitative analysis to show the differences between chains of materials. Any change in orderings and regularity of chains can be observed in XRD patterns. The structure of polymeric and carbonized Novolac was characterized in Figs. 13 and 14 using XRD patterns. According to pattern of Fig. 13 polymeric sample shows amorphous structure with a broad amorphous peak around 20°. this peaks is a characteristic peak of Novolac [29, 34].

Carbonization shows great change in cristallinity of samples. Fig. 14 reveals relatively two wide peaks in 25° and 45° which are definitely close to peaks of graphite and shows the pyrolysis at relatively high temperature [35, 36] subsequently dried at 100 °C and carbonized at 500 °C under nitrogen environment. The structure, morphology and performance of the membranes were examined by scanning electron microscopy (SEM).

Fig. 14 shows reflections around 21° and 24° which reveals increasing in d-spacing of material. The presence of reflection around 45°, 43° and 36° represent the carbon bond of graphite and demonstrate the ordered structure.

CONCLUSION

Supported carbon membranes were successfully fabricated on porous carbon supports. Both support and selective layers were fabricated from the same precursor. FE-SEM images and experimental gas test results revealed that a high quality carbon membrane could be prepared by coating of 40 wt% NPR mixed with CNT on carbonic support, which is suitable for gas separations. A high performance support was produced from 40 wt% NPR and 60 wt% activated carbon, and finally CO₂/CH₄ and CO₂/N₂ selectivity values of more than 17 were attained from C40M carbon membrane.

CONFLICT OF INTEREST

The authors declare that there is no conflict of interests regarding the publication of this manuscript.

REFERENCES

- [1] Nejad M. N., Asghari M., Afsari M., (2016), Investigation of Carbon nanotubes in mixed matrix membranes for gas separation: A review. *Chem. Bio. Eng. Rev.* 3: 276-298.
- [2] Article O., (2017), Effect of nano Zinc Oxide on gas permeation through mixed matrix Poly (Amide-6-b-Ethylene Oxide)-based membranes. *Int. J. Nano Dimens.* 8: 31-39.
- [3] Esmaeili N., Kazemian H., Bastani D., (2011), Synthesis of nano particles of LTA zeolite by means of microemulsion technique. *Iranian J. Chem. Chem. Eng.* 30: 1–8.
- [4] Kazemzadeh A., Bayati B., Kalantari N., (2012), Tubular MFI zeolite membranes made by in-situ crystallization. *Iran J. Chem. Chem. Eng.* 31: 37-44.
- [5] Scholes C. A., Stevens G. W., Kentish S. E., (2012), Membrane gas separation applications in natural gas processing. *Fuel.* 96: 15-28.
- [6] Barbosa-Coutinho E., Salim V. M. M., Borges C. P., (2003), Preparation of carbon hollow fiber membranes by pyrolysis of polyetherimide. *Carbon N. Y.* 41: 1707-1714.
- [7] David L. I. B., Ismail A. F., (2003), Influence of the thermastabilization process and soak time during pyrolysis process on the polyacrylonitrile carbon membranes for O₂/N₂ separation. *J. Memb. Sci.* 213: 285–291.
- [8] Asadi S. Z., Shekarian E., Tarighaleslami A. H., (2015), Preparation and characterization of nano-porous Polyacrylonitrile (PAN) membranes with hydrophilic surface. *Int. J. Nano Dimens.* 6: 217–226.
- [9] Centeno T. A., Fuertes A. B., (2001), Carbon molecular sieve membranes derived from a phenolicresin supported on porous ceramic tubes. *Sep. Purif. Technol.* 25: 379–384.
- [10] Wei W., Qin G., Hu H., (2007), Preparation of supported carbon molecular sieve membrane from novolac phenol-formaldehyde resin. *J. Memb. Sci.* 303: 80–85.
- [11] Suda H., Haraya K., (1997), Gas permeation through micropores of Carbon molecular sieve membranes derived from Kapton Polyimide. *J. Phys. Chem. B.* 101: 3988–3994.
- [12] Kalantari H., Yaghmaei S., Roostaazad R., (2014), Removal of zirconium from aqueous solution by *Aspergillus niger*. *Sci. Iran Trans. C. Chem. Chem. Eng.* 21: 772-776.
- [13] Liang C., Sha G., Guo S., (1999), Carbon membrane for gas separation derived from coal tar pitch. *Carbon N. Y.* 37: 1391–1397.
- [14] Steriotis T., Beltsios K., Mitropoulos A. C., (1997), On the structure of an asymmetric carbon membrane with a novolac resin precursor. *J. Appl. Polym. Sci.* 64: 2323–2345.
- [15] Shusen W., Meiyun Z., Zhizhong W., (1996), Asymmetric molecular sieve carbon membranes. *J. Memb. Sci.* 109: 267–270.
- [16] Habibzare S., Asgari M., Djirsarai A., (2014), Nano composite PEBAX®/PEG membranes: Effect of MWNT filler on CO₂/CH₄ separation. *Int. J. Nano Dimens.* 5: 247–254.
- [17] Mastali N., Bakhtiari H., (2013), Investigation on the structural, morphological and photochemical properties of spin-coated TiO₂ and ZnO thin films prepared by sol-gel method. *Int. J. Nano Dimens.* 5: 113–121.
- [18] Yampolskii Y., Freeman B., (2010), Membrane Gas Separation *Gas separation* membranes offer a number of benefits over other separation technologies, John Wiley & Sons, Ltd.
- [19] Mahmoudi A., Namdari M., Zargar V., (2014), Nano composite PEBAX® membranes: Effect of zeolite X filler on CO₂ permeation. *Int. J. Nano Dimens.* 5: 83-89.
- [20] Thommes M., Kaneko K., Neimark A. V., (2015), Physisorption of gases, with special reference to the evaluation of surface area and pore size distribution (IUPAC Technical Report). *Pure Appl. Chem.* 87: 1051–1069.
- [21] Li S., Fan C. Q., (2010), High-Flux SAPO-34 Membrane for CO₂/N₂ Separation. *Ind. Eng. Chem. Res.* 49: 4399–4404.
- [22] Grainger D., Hägg M. B., (2007), Evaluation of cellulose-derived carbon molecular sieve membranes for hydrogen separation from light hydrocarbons. *J. Memb. Sci.* 306: 307–317.
- [23] Sebastian V., Kumakiri I., Bredesen R., (2007), Zeolite membrane for CO₂ removal: Operating at high pressure. *J. Memb. Sci.* 292: 92–97.
- [24] Sircar S., Rao M. B., Thaeon C. M. A., (1999), Selective surface flow membrane for gas separation. *Sep. Sci. Technol.* 34: 2081–2093.
- [25] Huang D. S., Yi Z. Z., Huang Z. L., (2012), Mass transfer mechanism and mathematical model for extraction process of L-Theanine across bulk liquid membrane. *Iran. J. Chem. Chem. Eng.* 31: 53–58.
- [26] Allahbakhsh A., Bahramian A. R., (2016), Novolac-derived carbon aerogels pyrolyzed at high temperatures: Experimental and theoretical studies. *RSC Adv.* 6: 72777–72790.
- [27] Khalaj M., Allahbakhsh A., Bahramian A. R., (2017), Structural, mechanical and thermal behaviors of novolac/graphene oxide nanocomposite aerogels. *J. Non. Cryst. Solids.* 460: 19-28.
- [28] Yuan F.-Y., Zhang H.-B., Li X., (2014), In situ chemical reduction and functionalization of graphene oxide for electrically conductive phenol formaldehyde composites. *Carbon N. Y.* 68: 653–661.
- [29] Noparvar-Qarebagh A., Roghani-Mamaqani H., Salami-Kalajahi M., (2015), Functionalization of carbon nanotubes by furfuryl alcohol moieties for preparation of novolac phenolic resin composites with high carbon yield values. *Colloid Polym. Sci.* 293: 3623–3631.
- [30] Yeh M.-K., Tai N.-H., Liu J.-H., (2006), Mechanical behavior of phenolic-based composites reinforced with multi-walled carbon nanotubes. *Carbon N. Y.* 44: 1–9.
- [31] Noparvar-Qarebagh A., Roghani-Mamaqani H., Salami-Kalajahi M., (2017), Nanohybrids of novolac phenolic resin and carbon nanotube-containing silica network: Two different approaches for improving thermal properties of resin. *J. Therm. Anal. Calorim.* 128: 1027–1037.
- [32] Noparvar-Qarebagh A., Roghani-Mamaqani H., Salami-

- Kalajahi M., (2016), Novolac phenolic resin and graphene aerogel organic-inorganic nanohybrids: High carbon yields by resin modification and its incorporation into aerogel network. *Polym. Degrad. Stab.* 124: 1-14.
- [33] Ouchi K., (1966), Infra-red study of structural changes during the pyrolysis of a phenol-formaldehyde resin. *Carbon N. Y.* 4: 59-66.
- [34] Dante R. C., Santamaria D. A., Gil J. M., (2009), Crosslinking and thermal stability of thermosets based on novolak and melamine. *J. Appl. Polym. Sci.* 114: 4059-4065.
- [35] Llosa Tanco M. A., Pacheco Tanaka D. A., Rodrigues S. C., (2015), Composite-alumina-carbon molecular sieve membranes prepared from novolac resin and boehmite. Part I: Preparation, characterization and gas permeation studies. *Int. J. Hydrogen Energy.* 40: 5653–5663.
- [36] Hussain R., Qadeer R., Ahmad M., (2000), X-ray diffraction study of heat-treated graphitized and ungraphitized carbon. *Turkish J. Chem.* 24: 177-183.